

Heat Transfer and Pressure Drop Of Two-Phase Flow across Tube Bundles

Xuejing He¹, Zhenlin Li^{1*}, Ji Wang^{1*}

¹College of Mechanical and Transportation Engineering, China University of Petroleum (Beijing), Beijing 102249, China
2021310311@student.cup.edu.cn; zhenlinli@263.net; wangji@cup.edu.cn

Abstract - The refrigerant two-phase flow across tube bundles is widely used. Its heat transfer mechanism needs to be further studied. An experimental system was established for measuring heat transfer coefficients, pressure drop and observing flow patterns. The test section of tube bundles was designed. R1233zd as a new environmentally friendly refrigerant was used as the working fluid. The effects of vapor quality, heat flux and mass flow rate on heat transfer and pressure drop were analyzed. The falling film flow, bubbly flow and shear flow were observed. With the increasing vapor quality and heat flux, the heat transfer coefficient increases. With the increasing vapor quality and mass flow rate, the pressure drop increases.

Keywords: heat transfer; two-phase flow; pressure drop; tube bundles; R1233zd

1. Introduction

The tube bundle heat exchangers are widely used in seawater desalination [1, 2], liquefied natural gas (LNG) plants and chemical industry [3] due to its various advantages, such as higher heat transfer coefficient, compact structure, high pressure tolerance, [4] and lower refrigerant charge [5]. The heat exchanger is the main equipment that affects the heat transfer efficiency of the industry. Therefore, it is important to study the heat transfer and pressure drop of outside tube heat exchanger for improving the heat transfer efficiency and economic benefit.

Many researchers have experimentally studied heat transfer outside tubes. They used water as working fluid. Yue et al. [6] studied heat transfer outside tube. They found local heat transfer coefficient decreases firstly and then increases from upstream to downstream along the longitudinal tube bundles. Liu et al. [7] studied the effects of spray density, fluid temperature and tube spacing on local heat transfer coefficient along the tube surface. They considered that the tube surface has the impingement zone, the heat diffusion transfer zone and the tail detachment zone, where has different effects on heat transfer. Gui et al. [8] studied the effects of mass flux, pressure and thermodynamic quality for pressure drop. They found that the frictional pressure drop increases nearly linear with the increasing thermodynamic quality. The frictional pressure drop increases obviously with decreasing pressure and increasing mass flux due to the varying physical properties and velocity, and a correlation was given.

Some researchers numerically studied heat transfer and pressure drop for outside tube due to the development of CFD technology. They used air, water, oily wastewater as working fluid. Li et al. [9] studied the effects of geometric parameters for heat transfer and pressure drop across twisted oval tube bundles. They found the staggered tube layout has higher heat transfer performance compared with in line tube layout. Ma et al. [10] used Euler-Lagrange method to study heat transfer outside staggered tube bundles, and analyzed the influence of operation parameters on heat transfer. Meng et al. [11] used VOF (Volume of Fluid) method to study the effect of tube arrangement, structural parameters on flow pattern and heat transfer for inline tube bundles and triangle tube bundles. Moerloose et al. [12] proposed a new model and studied forces working on two-phase flows in tube bundles. Most researchers studied the heat transfer and pressure drop for different working fluid. However, further research is still needed on heat transfer and pressure drop for new environmental-friendly refrigerant across tube bundles.

In the present study, the flow pattern observation, heat transfer coefficient and pressure drop measurement of R1233zd were experimentally carried out. The heat transfer and pressure drop of R1233zd flowing across tube bundles were analyzed.

2. Experimental rig and conditions

2.1 Experimental rig

The schematic diagram of the experimental setup is shown in Fig. 1. The experimental system is subdivided into two parts, including a refrigerant loop and a cooling water loop.

The main experimental equipment included a pump, mass flow meter, evaporator, dry filter, test section, fast camera, post condenser, thermostatic water bath and liquid reservoir. The working fluid comes out from the liquid reservoir. The pump was used to control the mass flow rate, which was measured by mass flow meter and controlled by regulating valve. Then the working fluid flows into evaporator, where the fluid reaches a vapor quality range from 0.1-0.9. Then the working fluid flows through the test section. After flowing out of the test section, the working fluid enters the post condenser and be condensed into sub-cooled liquid. Then it flows back into the liquid reservoir.

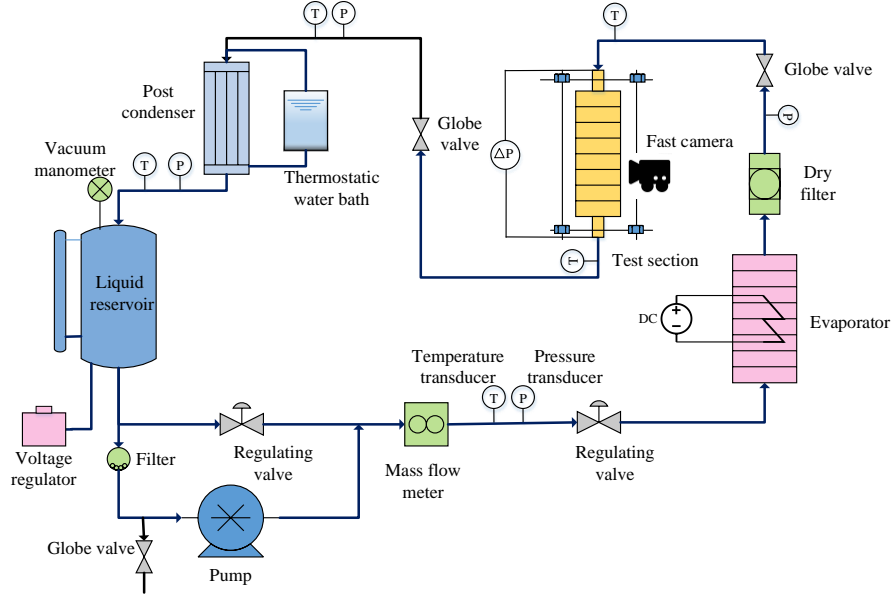


Fig. 1. Schematic diagram of experimental setup

The test section is shown in Fig. 2. The outer diameter of the tube is 12.0 mm. The radial tube pitch is 14.0 mm. The longitudinal tube pitch is 16.0 mm. The test section has 10 rows of tubes. Pressure drop was measured by pressure difference transducer. Temperature was measured by Platinum resistance temperature sensor.

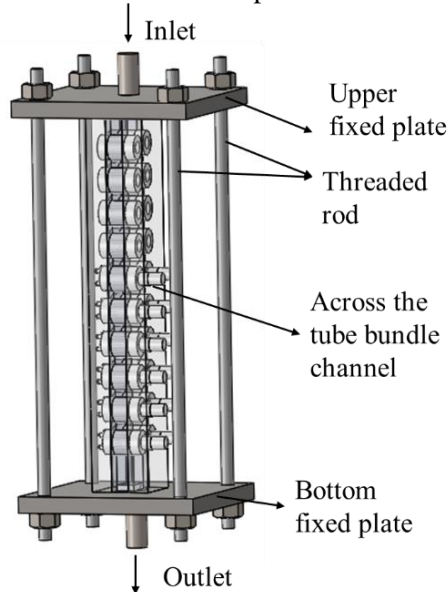


Fig. 2 Test section

2.2 Experimental conditions

The experimental fluid was R1233zd. The vapor quality was 0.1-0.9. The mass flow rate was 3kg/h and 4kg/h. The heat flux was 3000-5000 W/m² as shown in Table 1.

Table 1 Experimental conditions.

| Parameter | Value |
|----------------|--|
| Fluid | R1233zd |
| Vapor quality | 0.1, 0.2, 0.3, 0.4, 0.5, 0.6, 0.7, 0.8, 0.9 |
| Mass flow rate | 3 kg/h, 4 kg/h |
| Heat flux | 3000W/m ² , 5000W/m ² , 7000W/m ² |

3 Data reduction and uncertainty analysis

3.1 Data reduction

The local heat transfer coefficients are given by:

$$h = \frac{q}{\left(T_w - \frac{T_{in} + T_{out}}{2} \right)} \quad (1)$$

$$q = \frac{Q}{4 \cdot (2\pi R_{in} \cdot L_h)} \quad (2)$$

where, q is heat flux. T_{in} and T_{out} are temperature of inlet and outlet experimental section. Q is the electrical power of the test section. T_w is outer tube wall temperature. R_{in} is the distance between the thermocouple location and the heated tube center. L_h is length of heating rod.

The local frictional pressure drop are given by:

$$\Delta P_t = \Delta P_f + \Delta P_g + \Delta P_{con} + \Delta P_{ex} + \Delta P_{ac} \quad (3)$$

where, ΔP_t is the total pressure drop; ΔP_f is the frictional pressure drop; ΔP_g is the gravity pressure drop; ΔP_{ac} is the acceleration pressure drop; ΔP_{con} is the contraction pressure drop; ΔP_{ex} is the expansion pressure drop.

3.2 Uncertainty analysis

The uncertainty was given by Moffat [13].

$$\delta R = \left[\sum_{i=1}^N \left(\frac{\partial R}{\partial V} \delta V_i \right)^2 \right]^{1/2} \quad (4)$$

where, δR is the uncertainty of parameter R , V is the variable that affects the uncertainty of parameter R , δV is the uncertainty of parameter V .

4 Experiment results and discussion

4.1 Flow pattern observation

The fast camera was used to observe the flow pattern in the test section. Various flow patterns were presented in Fig. 3. The falling film flow, bubbly flow, shear flow are observed with increasing vapor quality. The falling film flow presents a

whole film and covers the wall surface, which is a continuous liquid film between the tubes as shown in Fig. 3(a). The bubble flow looks like liquid and bubbles mixed between the tubes as shown in Fig. 3(b). For the shear flow as shown in Fig. 3(c), the liquid film was broken by gas flow, and the liquid is entrained into the gas.

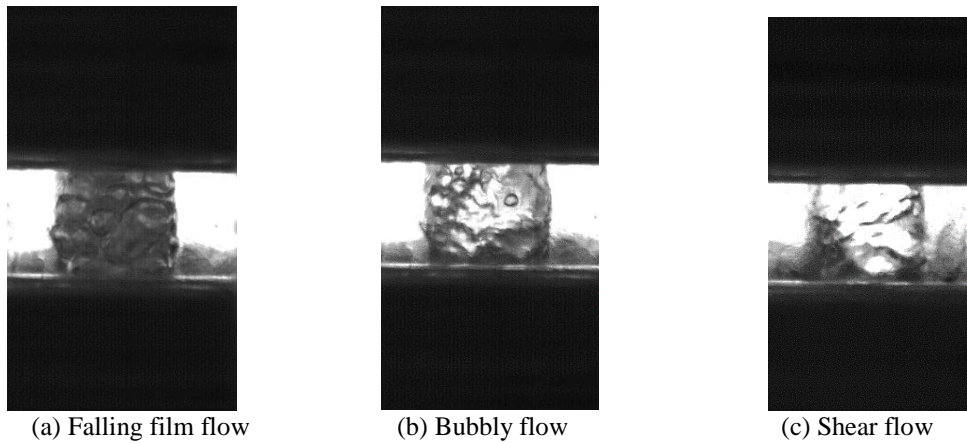


Fig. 3. Flow patterns

4.2 Heat transfer characteristics

The experimental heat transfer coefficients are shown in Fig. 4. The heat transfer coefficient increased continuously with increasing vapor quality. As the vapor quality increases, the velocity of liquid film increases due to increasing shear stress, resulting in stronger convective heat transfer. Therefore, the heat transfer coefficient increased. The heat transfer coefficient increases with increasing heat flux. The heat flux increases, resulting in increasing nucleate boiling and higher heat transfer.

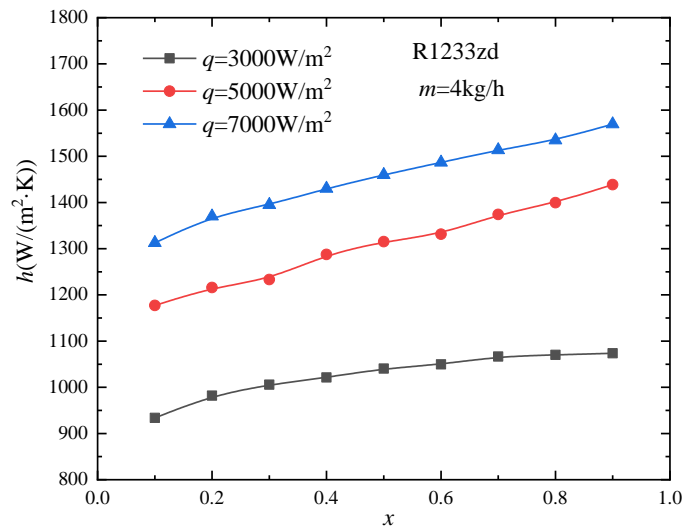


Fig. 4. Experimental heat transfer coefficients

4.3 Pressure drop characteristics

The experimental pressure drops for various vapor qualities and mass flow rates are shown in Fig. 5. The frictional pressure drop increases with increasing vapor quality and mass flow rate. With increasing vapor quality, the relative velocity of gas and liquid increases, causing higher shear stress. Therefore, the frictional pressure drop increases due to increasing friction force. With increasing mass flow rate, the gas and liquid mass flow rate both increases and resulting in increasing gas-liquid shear stress. Therefore, the frictional pressure drop increased.

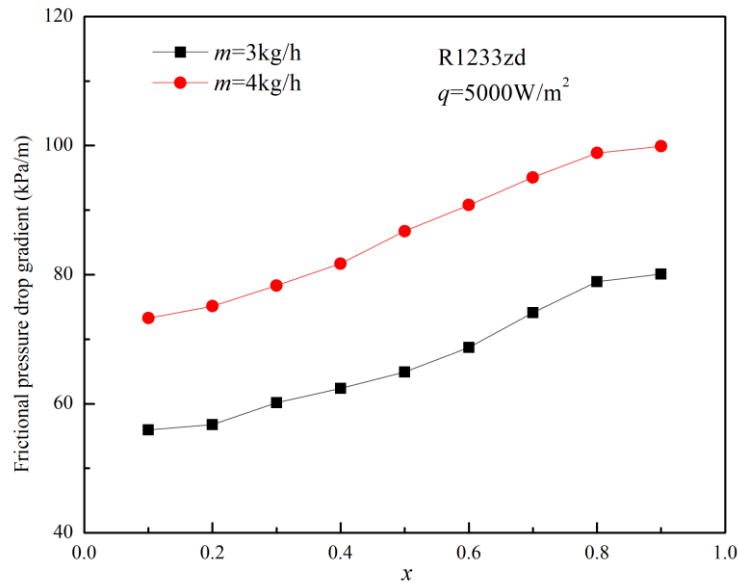


Fig. 5. Experimental pressure drop

Conclusion

(1) The flow patterns across tube bundles including falling film flow, bubbly flow and shear flow were observed as the vapor quality increases from 0.1 to 0.9.

(2) With increasing vapor quality, the heat transfer coefficient across tube bundles increases due to increasing convective heat transfer. With increasing heat flux, the bubbly flow appears, promoting nucleate boiling heat transfer, while heat transfer coefficient across tube bundles increases.

(3) The frictional pressure drop across tube bundles increases with increasing vapor quality and mass flow rate due to higher shear stress.

Acknowledgements

This work is supported by National Natural Science Foundation of China (Grant52006242), National Natural Science Foundation of China (Grant 52192623)

References

- [1] S. Shen, Y. Guo, L. Gong, "Analysis of heat transfer critical point in LT-MEE desalination plant," *Desalination* 432 (2018) 64–71.
- [2] Y. Ghalavanda, M.S. Hatamipoura, A. Rahimia, "A review on energy consumption of desalination processes," *Desalination and Water Treatment*. 54 (2015)1526–1541.
- [3] Y. Zheng, X. Ma, Y. Li, R. Jiang, K. Wang, Z. Lan, Q. Liang, "Experimental study of falling film evaporation heat transfer on super hydrophilic horizontal-tubes at low spray density," *Applied Thermal Engineering*. 111 (2017) 1548–1556.
- [4] X.J He, J. Wang, Z.L. Li, R. Wan, J. Hu, Z.M. Yang. "Numerical simulation on shell-side flow pattern transition and heat transfer of non-azeotropic refrigerant mixture," *Applied Thermal Engineering* 214 (2022) 118917.
- [5] H. Han, S.W. Wang, Y.X. Li, C.Z. Sun, "3-D Numerical study for the film thickness distribution of n-pentane falling film flow around the curved egg-shaped tube bundle," *Chemical Engineering Research and Design*. 156(2020)156–170.

- [6] Y.K. Yue, J.L. Yang, X.Q. Li, Y.C. Song, Y. Zhang, Z.T. Zhang. “Experimental research on falling film flow and heat transfer characteristics outside the vertical tube”, *Applied Thermal Engineering* 199 (2021) 117592.
- [7] S.L. Liu, X.S. Mu, S.Q. Shen, C. Li, B.Y. Wang. “Experimental study on the distribution of local heat transfer coefficient of falling film heat transfer outside horizontal tube”, *International Journal of Heat and Mass Transfer* 170 (2021) 121031.
- [8] M. Gui , Q.C. Bi , Teng Wang, , J.Q. Shan, et.al, “Experimental investigation on pressure drop characteristics of two-phase flow in a rod bundle geometry under high pressure conditions”, *Annals of Nuclear Energy* 165 (2022) 108787.
- [9] X.Z. Li , D.S. Zhu , Y.D. Yin, A. Tu, S. Liu, “Parametric study on heat transfer and pressure drop of twisted oval tube bundle with in line layout,” *International Journal of Heat and Mass Transfer* 135 (2019) 860–872.
- [10] H.Q. Ma, Y.M. Liu, Y. Xie, Y. Liu, R.X. Ding, C.Q. Hou, X.M. Luo, Z.X. Lei, “Numerical investigation on heat-mass transfer and correlations of humid air-water outside staggered tube bundles”, *International Journal of Thermal Sciences* 179 (2022) 107632.
- [11] S. Meng, Z. He, T. He, N. Mao, “Influence of horizontal tube bundle arrangement on flow and heat transfer properties of oily wastewater spray falling film” *Applied Thermal Engineering* 225 (2023) 120177
- [12] L. Moerlose, A. Bral, T. Demeester, M. Paepe, J. Degroote,” Effect of a new synthetic bubble model on forces in simulations of two-phase flows in tube bundles”, *European Journal of Mechanics / B Fluids* 90 (2021) 49–62
- [13] R.J. Moffat. “Describing the uncertainties in experimental results,” *Experimental Thermal And Fluid Science*, 1988, 1(1): 3-17